Experimental Study of the Plume Impingement Problem Associated with Rocket Stage Separation

J. Allègre* and M. Raffin*
Société d'Etudes de Constructions et de Services pour Souffleries et Installations Aérothermodynamiques Meudon, France
and
J.C. Lengrand†
Centre National de la Recherche Scientifique, Meudon, France

Experiments are carried out to quantify interaction effects due to retrorocket plume impingement on Ariane launcher upper stages. Wall pressure measurements, combined with density surveys and flowfield visualization, give useful information on the flow structure in the vicinity of the payload. Wall pressure data obtained in simulation conditions are converted into real flight values by applying an approximate transportation method. Another configuration is also presented where the shock, induced by the plume/launcher interaction, intersects antennas located perpendicular to the launcher wall. The shock impingement induces high levels of local heat fluxes.

Nomenclature

C	= Chapman-Rubesin constant
c_p	= specific heat at constant pressure
h	= nozzle-plate normal distance
I	= jet similarity parameter
p	= pressure
p_N, p_∞, p_w	= Newtonian, ambient, and wall pressure, respectively
q	= heat flux
r_c, r_e	= nozzle throat and exit radii, respectively
r_{MD}	= Mach disk distance
Re_c	= critical Reynolds number based on initial diameter
Re_h	= defined as $Re_c r_c/h$
T	= temperature
T_0, T_w	= stagnation and wall temperatures, respectively
U_L	= limiting velocity
γ	= ratio of specific heats
δ^*	= boundary-layer displacement thickness
θ	= polar angle
θ_∞	= maximum angle of jet boundary
ρ, ρ_0	= local and stagnation density, respectively
τ	= skin friction

Introduction

WHEN a rocket engine is fired at high altitude, exhaust gases expand into a large solid angle, and impingement on nearby surfaces cannot be avoided. Examples of situations in which this problem is encountered on board spacecraft are: the operation of stabilization or maneuver thrusters, multiple satellite launching, launching from a reusable spacecraft and launcher stage separation. Undesirable consequences of exhaust plume impingement include additional forces and torques exerted on the spacecraft, surface heating, contamination[1] (with possible damage to solar cells, optics and antennas), and electrical charging.

Theoretical predictions of impingement flowfields and surface flux quantities have been attempted both by "exact" and "semiempirical" methods.

Exact methods include: 1) Monte Carlo direct simulation under rarefied conditions, even for complex geometries;[2] and 2) solving the continuum flow equations for simple impingement configurations.[3]

Semiempirical methods[4-6] consist in a local treatment of the plume surface interaction. They have proved to be sufficiently accurate for engineering purposes in the determination of heat transfer and the tangential force to a flat plate impinged upon by a plume.[4,5] Unfortunately, they do not predict correctly the surface pressure distribution but give only the correct order of magnitude of the pressure peak.[7] Furthermore, they are restricted to simple surface geometries.

The present work is devoted to the impingement problem associated with Ariane launcher's stage separation. When the second stage separates, retrorockets are fired during approximately one s. Exhaust gases impinge on the cylindrical wall of the second and third stages, and possibly upon the payload itself (Fig. 1). Heat transfer to the launcher wall and to the payload has been studied in a previous work.[8] Both heat-transfer and surface pressure distributions have now been obtained, as well as flowfield visualizations and density con-

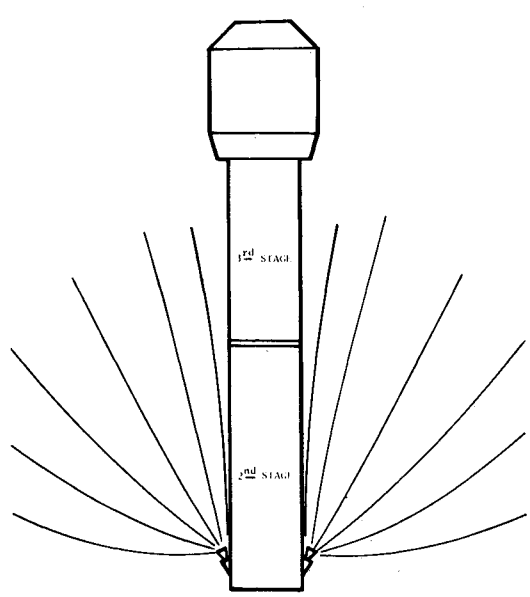

Fig. 1 Ariane configuration with plume due to retrorocket firing.

Presented as Paper 85-0930 at the AIAA 20th Thermophysics Conference, Williamsburg, VA, June 19-21, 1985; revision received Nov. 30, 1985.

*Research Engineers.

†Research Scientist, Laboratoire d'Aérothermique.

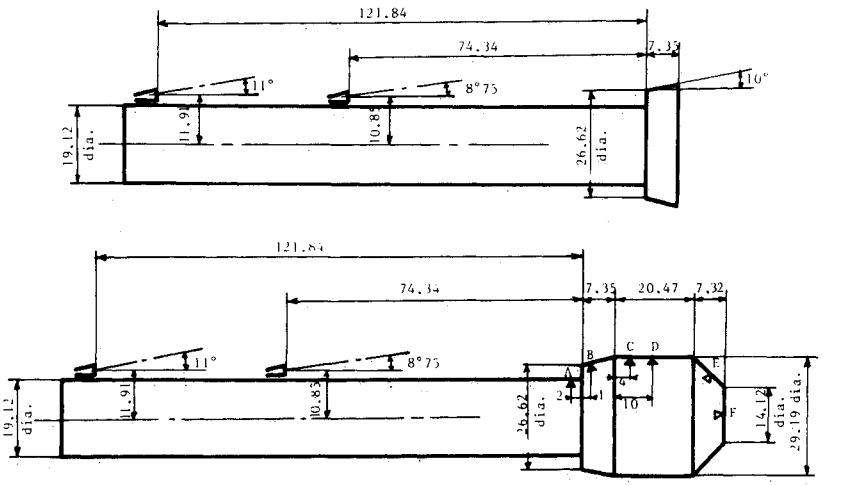

Fig. 2 1/36 scale-model geometries.

tours. The high nozzle Reynolds number and the proximity of the impinged surfaces caused the flow to be in the continuum or near-continuum regime, where theoretical predictions are difficult to obtain. The present work is therefore essentially experimental in nature.

Experimental Setup

Experiments were carried out in the SR3 vacuum chamber of the Laboratoire d'Aérothermique at Meudon. A 1/136-scale model of the launcher's upper stages was located in the vicinity of a nozzle representative of a retrorocket. A "short" and a "long" configuration were used to simulate two possible locations of the retrorocket on the second stage. Also, two possible configurations of the payload supporting system were investigated (Fig. 2).

Heat fluxes were also measured on antennas located perpendicular to the surface of the launcher wall.

The nitrogen plume simulating the retrorocket plume was generated by an underexpanded nozzle with an exit Mach number of 2.45. Stagnation conditions, nozzle geometry, and flow conditions are summarized in Table 1. Full-scale conditions are also presented in Table 1. The wind-tunnel pumping system allowed continuous operation of the nozzle, at a fixed vacuum chamber pressure, without time limitation.

Experiments included: flowfield density measurements and flowfield visualization using the electron beam fluorescence technique, wall pressure measurements using differential pressure transducers, and heat-transfer measurements using the thermosensitive paint technique.

Transposition from Simulation to Real-Flight Conditions

During the simulation, model size, gas nature, and nozzle stagnation conditions are different from real-flight values; therefore, full-scale quantities have to be deduced from the corresponding quantities measured during simulation tests.

Data transposition is made with the following procedure: 1) the same theoretical model is used to calculate the quantities of interest under both simulation and real-flight conditions; 2) the ratio between real-flight and simulation calculated results is then applied to the simulation experimental results to predict the real-flight values.

Simulation conditions have to be adequately chosen in order to simulate properly the most significant governing parameters. This requires both dimensional analysis and physical considerations.[9] For a given geometry of impinged surfaces, the impingement process is governed by parameters related to nozzle working conditions and geometry, working and ambient gas properties, and impinged surface characteristics.

An approximate theoretical model has been developed to calculate plume quantities,[10] wall heat transfer,[4] wall pressure, and wall shear stress[5] on collision surfaces.

Table 1 Nozzle conditions

	Full-scale conditions	Simulation conditions
Stagnation conditions		
Pressure, Pa	$123\ 10^5$	$4\ 10^5$
Temperature, K	3150	1100
Nozzle geometry		
Throat radius, m	$20.55\ 10^{-3}$	$0.8\ 10^{-3}$
Exit radius, m	$81\ 10^{-3}$	$1.3\ 10^{-3}$
Half-angle of divergence, deg	6	10
Nozzle flow		
Throat Reynolds number, based on diameter	$4.60\ 10^6$	$2.04\ 10^4$
Mass-flow rate, kg/s	10.57	$0.96\ 10^{-3}$
Thrust, N	$29.12\ 10^3$	1.18
Exit conditions		
Relative boundary-layer displacement thickness δ^*/r_e	$4.19\ 10^{-3}$	$2.39\ 10^{-2}$
Mach number	3.61	2.45
Density distribution parameter I	0.187	0.204

The hypotheses suppose that: 1) the background pressure is zero; 2) the impingement occurs at large distances from the nozzle, the nozzle appearing like a source point; 3) continuum regime concepts remain valid; 4) the impingement involves only the central part of the jet; and 5) the impinged surface geometry is not too complex.

With the above, the model indicates that 1) the distribution of wall pressure $p/p_{N\text{ref}}$ is a function of I only, where

$$I = 0.613[(\gamma-1)/2]^{0.835}[\theta_\infty/(\pi/2)]^{1.92}$$

I characterizes the angular density distribution within the jet; 2) distributions of skin friction $\tau/p_{N\text{ref}}$ and heat transfer q/q_{ref} are functions of I, with a weak influence of γ and T_w/T_0, and a negligible influence of other parameters.

Expressions of $p_{N\text{ref}}$ and q_{ref} are:

$$p_{N\text{ref}} = 0.978[(\gamma-1)/2]^{-0.337} p_0 \left(\frac{r_c}{h}\right)^2$$

$$q_{\text{ref}} = \rho_0 U_L \left(\frac{r_c}{h}\right)^2 c_p (T_0 - T_w) C^{-0.5} Re_h^{-0.5}$$

The conditions for correct simulation of the real impingement problem have been discussed.[9] The nozzle need not be at

the same scale as the spacecraft wall, provided it is sufficiently small to be considered as a source point under both simulation and full-scale conditions. It has not been possible to simulate properly the relative boundary-layer displacement thickness δ^*/r_e in the nozzle exit plane. This should induce only negligible error because δ^*/r_e is very small in both simulation and full-scale conditions and impingement involves only gas originating from the nozzle inviscid core rather than from the boundary layer. The density distribution parameter I was nearly the same under both simulation and full-scale conditions.

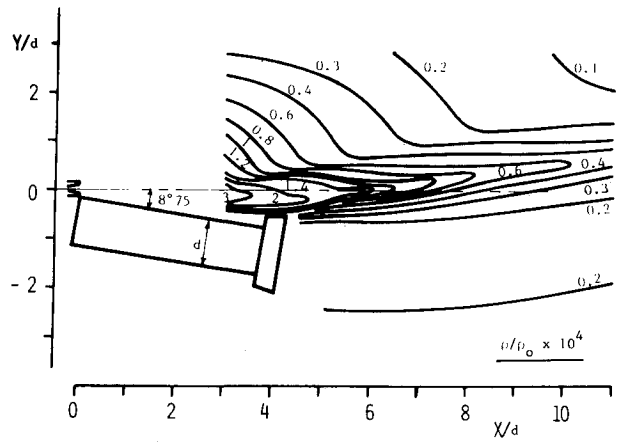

Fig. 3 Density flowfield; short cylindrical model ($P_\infty = 2.67$ Pa).

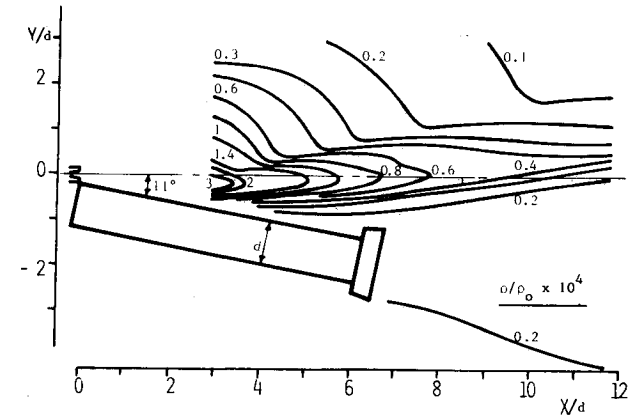

Fig. 4 Density flowfield; long cylindrical model ($P_\infty = 2.67$ Pa).

Plume Impingement with the Launcher

It is desirable that the background pressure be low enough for the jet size to be much larger than the model size. In the present experiments, two values of the background pressure were considered, 2.67 and 5.34 Pa. Both values were low enough for the Mach disk to be at a distance larger than three times the model size.

The density contours obtained in the plane of symmetry of the impingement region are presented in Figs. 3 and 4, respectively, for the short and long cylindrical models (Fig. 2); ρ and ρ_0 denote local and stagnation density, respectively. The value of the background pressure is 2.67 Pa. Flow visualization in Fig. 5 corresponds to the long cylindrical model. According to the jet model,[10] the reduced density ρ/ρ_0 at a given location in the full-scale flowfield is obtained by multiplying the value of ρ/ρ_0 at the corresponding location of the simulated flowfield by a factor of 0.029.

The effects of plume impingement on the wall may depend on the radius of curvature of the wall. In order to evidence the influence of the radius of curvature of the launcher stage, we compared the flowfield density distribution as shown in Fig. 4 with the flowfield density distribution of Fig. 6, where the cylindrical wall had been replaced by a two-dimensional wall having the same profile as the model and a virtually infinite span.

The increase of the wall curvature radius leads to a stronger interaction shock with a higher density level in the vicinity of the surface. The interaction shock is more distant from the model wall. One other possible configuration of the payload supporting system is shown in the second sketch of Fig. 2, and wall pressures were recorded for six points as indicated in the figure.

Wall pressures were investigated for short and long cylindrical models. For both configurations the two values 2.67 and 5.34 Pa of the background pressure were considered. For the short configuration (Fig. 7), the wall pressure is independent of the background pressure except on the rear-facing surface. The high levels of measured pressures in the vicinity of the upstream side of the payload supporting system point out the strong interaction process in this region. For the long configuration (Fig. 8), the wall pressure is affected by the external pressure level for all points considered. At the highest external pressure level, this indicates that the simulation is not correct enough to yield quantitative values of wall pressure for real-flight conditions.

Calculations based on the transposition method, as discussed in the previous paragraph, indicated that a factor of 40.9 had to be applied to wind-tunnel wall pressure data to yield the real-flight wall pressure. All results presented here refer to simulation conditions.

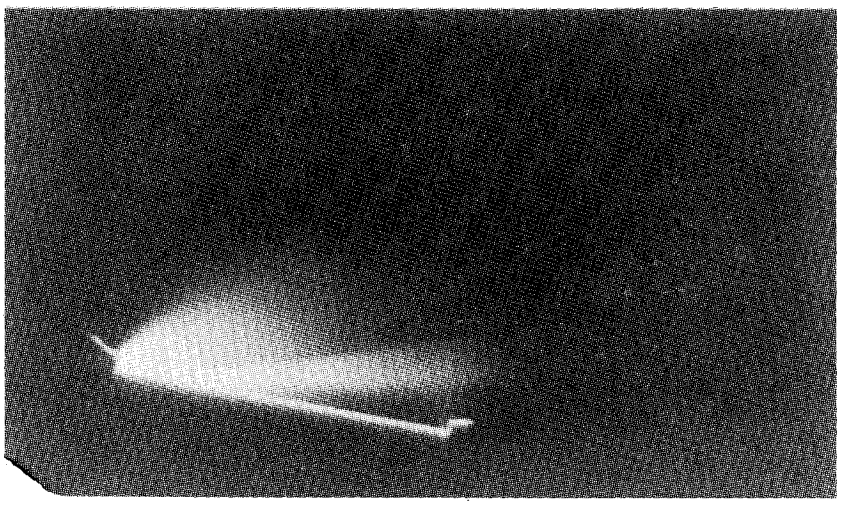

Fig. 5 Flow visualization; long cylindrical model ($P_\infty = 2.67$ Pa).

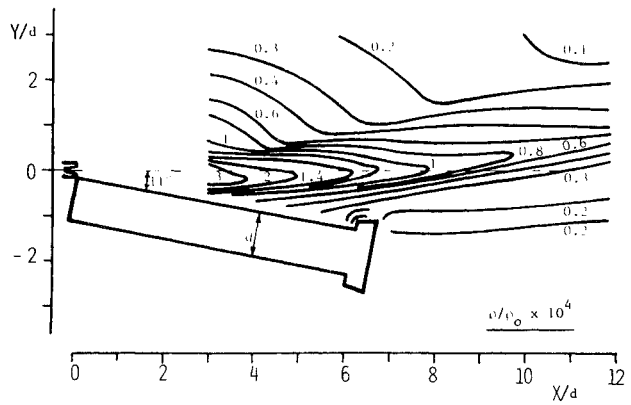

Fig. 6 Density flowfield; long flat model ($P_\infty = 2.67$ Pa).

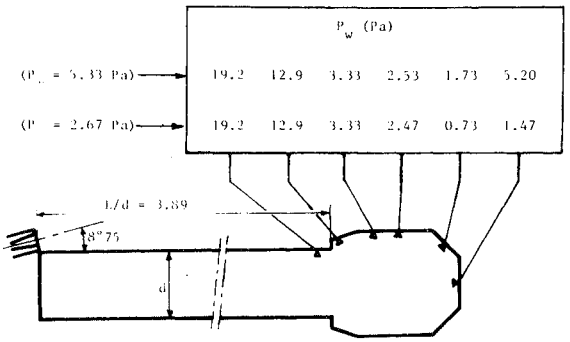

Fig. 7 Wall pressure on axisymmetric short-configuration model.

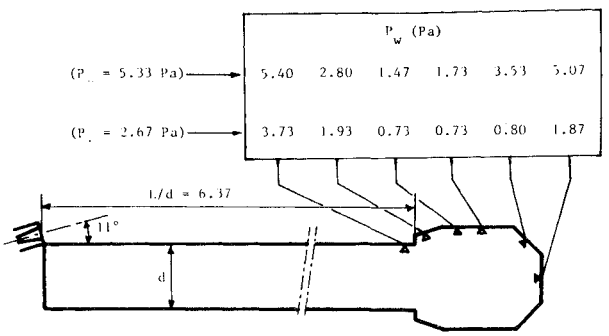

Fig. 8 Wall pressure on axisymmetric long-configuration model.

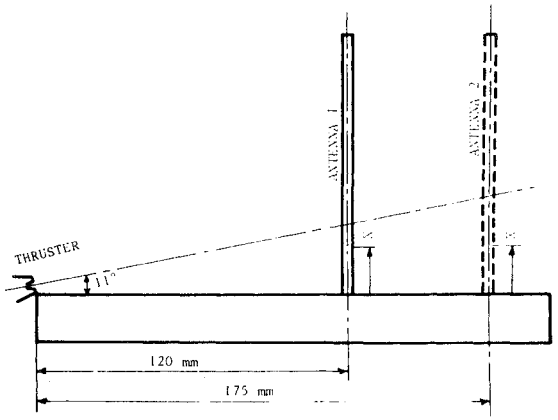

Fig. 9 Position of antennas 1 and 2 on the cylindrical model.

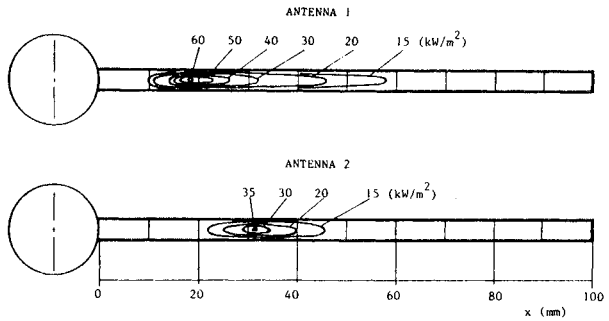

Fig. 10 Heat-transfer distribution on antennas 1 and 2.

Table 2 Maximum values of heat fluxes

	α, deg	11	20	30
q_{max}exp, kW/m²	Antenna 1	60	—	—
	Antenna 2	35	—	—
	Antenna 3	60	46	35
	Antenna 4	44	35	23

Plume Impingement on Antennas

Heat transfer has been measured on cylindrical antennas impinged on the interaction shock induced by the launcher wall. When it intersects an element of the spacecraft, the shock may cause an important local increase of the heat transfer to the element.

Heat-transfer measurements were performed by means of thermosensitive paint deposited on an insulating coating that covered the model surface. Preliminary calibration of the paint was carried out, using thermocouples embedded in a thin-wall plate. The model, initially shielded from plume heating, was introduced into the plume within a fraction of a second. A movie camera recorded the displacement of the lines of equal temperature at the surface of the model in order to deduce quantitative information on heat flux values.

The method was used to perform heat flux measurements on cylindrical antennas 4 mm in diameter and 100 mm long, submitted to the shock impingement, and disposed perpendicular to the surface of the launcher wall.

For the present tests, retrorocket flow conditions are indicated in Table 1, and the external pressure was 2.67 Pa.

Several distances along the launcher wall were considered. Figure 9 shows two positions of the antenna mounted successively at 120 mm (antenna 1) and 175 mm (antenna 2) downstream of the nozzle exit.

The angle α between the launcher wall and the thruster axis ranged from 11 to 30 deg. Experimental heat flux distributions for $\alpha = 11$ deg are presented in Fig. 10. As expected from the decrease of density vs abscissa, the heat flux decreases as abscissa increases. Maximum values of the heat fluxes are given in Table 2 for antennas 1 and 2.

For each value of incidence α, heat fluxes have also been measured on two cylindrical antennas located at a distance of 120 mm downstream of the thruster exit (Fig. 11). One antenna is mounted in the plane of symmetry that contains the launcher and thruster axes. The other antenna, inclined with an angle of 45 deg, is located in the same cross section. As an example, for $\alpha = 20$ deg Fig. 12 gives the heat-transfer distribution on the two antennas. Heat flux intensities are given in Table 2 for the three values of α considered, showing an important effect of the thruster incidence on the measured heat fluxes. If one considers the antenna located in the plane of symmetry, the maximum heat flux values are 60 kW/m² and 35 kW/m² for the respective incidences of 11 and 30 deg.

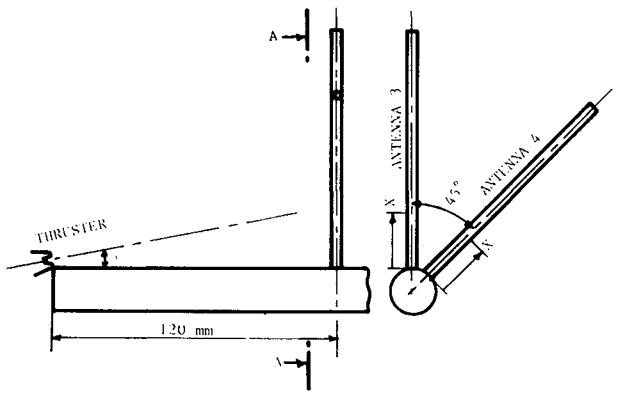

Fig. 11 Position of antennas 3 and 4 on the cylindrical model.

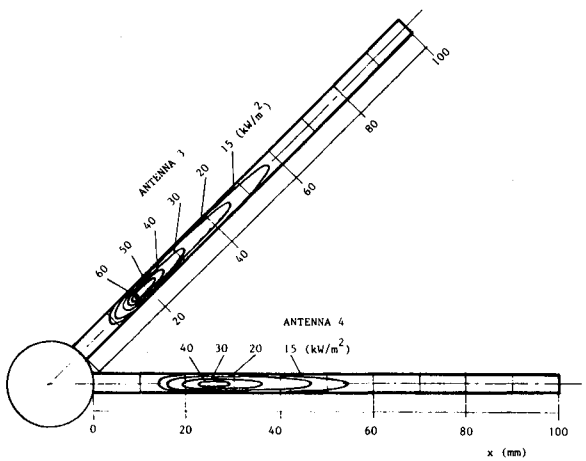

Fig. 12 Heat-transfer distribution on antennas 3 and 4.

This results from the attenuation of the interaction shock intensity with increasing values of α. Also, lower values of heat fluxes are recorded when the antenna is moved away from the plane of symmetry; the flux attenuation is of the order of 20% for an inclination of 45 deg of the antenna.

The theoretical treatment[5] allowing the calculation of heat fluxes for flight conditions from model simulation is inadequate when applied to interactions involving successive interactions with different surfaces. Consequently, no attempt was made to apply it to the present configuration.

Conclusion

Results concerning the plume impingement problem associated with the separation of the second stage of the Ariane launcher have been obtained through wind-tunnel experiments. They include flowfield visualizations and density measurements as well as pressure measurements. They have been converted into full-scale values useful for the spacecraft designer. They are available for further validation of theoretical models. The limitations of the simulation procedure due to the background pressure have been pointed out.

Heat flux measurements have been performed on cylindrical antennas mounted at different locations perpendicular to the launcher wall. The heat flux distribution is strongly affected by the interaction shock due to the presence of the launcher wall.

Acknowledgments

The authors gratefully acknowledge the financial support of the Centre National d'Etudes Spatiales (CNES) under Contract 83-3058.

References

[1]Trinks, H. and Hoffman, R.J., "Experimental Investigation of Bipropellant Exhaust Plume Flowfield, Heating and Contamination, and Comparison with the CONTAM Computer Model Predictions," AIAA Paper 83-1447, June 1983.

[2]Hueser, J.E., Melfi, L.T., Bird, G.A., and Brock, F.J., "Analysis of Large Solid Propellant Rocket Engine Exhaust Plumes Using the Direct Simulation Monte Carlo Method," AIAA Paper 84-0496, Jan. 1984.

[3]Sokolov, Y.I., and Uskov, V.N., "An Approach to Calculating the Flow Following Impingement of an Underexpanded Jet onto an Infinite Planar Baffle," *Fluid Mechanics, Soviet Research,* Vol. 10, 1981, pp. 105-115.

[4]Lengrand, J.C., Allegre, J., and Raffin, M., "Heat Transfer to a Surface Impinged Upon by a Simulated Rocket Exhaust Plume," *Progress in Astronautics and Aeronautics: Proceedings of the 12th Rarefied Gas Dynamics Symposium,* Vol. 74, edited by S.S. Fisher, AIAA, New York, 1981, Pt. II, p. 980.

[5]Allègre, J., Raffin, M., and Lengrand, J.C., "Forces Induced by a Simulated Rocket Exhaust Plume Impinging upon a Flat Plate," *Proceedings of the 14th Rarefied Gas Dynamics Symposium,* edited by H. Oguchi, Tsukuba, Japan, July 1984.

[6]Legge, H. and Boettcher, R.D., "Modelling Control Thruster Plume Flow and Impingement," *Proceedings of the 13th Rarefied Gas Dynamics Symposium,* Plenum Press, New York, 1985.

[7]Lengrand, J.C., Raffin, M., and Allègre, J., "Monte-Carlo Simulation Method Applied to Jet-Wall Interactions Under Rarefied Conditions," *Progress in Astronautics and Aeronautics: Proceedings of the 12th Rarefied Gas Dynamics Symposium,* edited by S.S. Fisher, Vol 74, 1981, pt. II, p. 994.

[8]Allègre, J., Raffin, M., and Lengrand, J.C., "Experimental Study of Plume Impingement and Heating on Ariane's Payload," *Proceedings of the 13th Rarefied Gas Dynamics Symposium,* Plenum Press, New York, 1985.

[9]Lengrand, J.C., "Plume Impingement upon Spacecraft Surfaces," *Proceedings of the 14th Rarefied Gas Dynamics Symposium,* edited by H. Oguchi, Tsukuba, Japan, July 1984.

[10]Lengrand, J.C., Allègre, J. and Raffin, M., "Underexpanded Free Jets and Their Interaction with Adjacent Surfaces," *AIAA Journal,* Vol 20, Jan. 1982, pp. 27-28.